Journal of Power Sources 195 (2010) 3984–3989

Contents lists available at ScienceDirect

Journal of Power Sources

journal homepage: www.elsevier.com/locate/jpowsour

Investigation of the oxygen reduction reaction on the carbon electrodes loaded with MnO_2 catalyst

Narah Ominde[a], Nick Bartlett[a,1], Xiao-Qing Yang[b], Deyang Qu[a,*]

[a] Department of Chemistry, University of Massachusetts Boston, 100 Morrissey Boulevard, Boston, MA 02125-3393, United States
[b] Chemistry Department, Brookhaven National Laboratory, Upton, NY 11973, United States

ARTICLE INFO

Article history:
Received 5 December 2009
Received in revised form
28 December 2009
Accepted 29 December 2009
Available online 13 January 2010

Keywords:
Oxygen reduction
Gas diffusion electrode
Manganese dioxide catalyst
Pore distribution

ABSTRACT

The oxygen reduction reaction has been studied on gas diffusion electrodes made with various activated carbon materials and on the edge/basal orientations of pyrolitic graphite. A MnO_2 catalyst was loaded on all carbon surfaces. The MnO_2 catalyst demonstrated significant catalytic activity for the oxygen reduction reaction. The specific catalytic activity was found to relate to the concentration of the edge orientation of carbon materials loaded with MnO_2 catalyst. The higher the percentage of edge orientations, the higher the specific catalytic activity would be. MnO_2 may not participate in the reduction of O_2, but catalyze the disproportionation of HO_2^-.

© 2010 Elsevier B.V. All rights reserved.

1. Introduction

There has been a persistent and continuous effort to search for clean and renewable power sources. Fast growing markets of electronic devices for both civilian and military applications require high energy battery systems. The rapid proliferation and commercial success of hybrid electric vehicles (HEVs) renewed the interest in the development of high capacity traction batteries to take HEVs to the next level of plug-in hybrid vehicles (PHEVs). PHEVs are believed to be the next generation of urban commuting vehicles, preceding the advent of true electric vehicles.

Metal–air cells, which utilize oxygen in the air as the cathode active material, provide high energy density. Air cathodes have been investigated for decades, and manganese oxides [1–10] have been identified as the most promising candidates for the oxygen reduction reaction (ORR) catalyst because of their low cost, abundance and environmental friendliness. However, the activity and mechanism by which the ORR takes place in these materials remain to be fully understood, even though the mechanism of the ORR catalyzed by manganese oxide has been extensively studied. It was proposed [11–15] that a manganese oxide catalyzed ORR goes through successive 2-electron processes. The intermediate HO_2^- species formed after oxygen gains two electrons disproportionate into O_2 and OH^- on the MnO_x sites. Manganese oxide was believed to be an efficient catalyst for HO_2^- disproportionation [12,15]. The reaction is sensitive to the percentage of manganese oxide in the carbon material and the types of manganese oxide [16]. The electrode containing a low percentage of manganese catalyst tends to follow the peroxide pathway, forming peroxide ions due to the fact that HO_2^- cannot effectively disproportionate [15]. Thus, insufficient catalyst can result in peroxide accumulation on the electrode surface and in the pores of GDL, it leads to a lower voltage and impedes the fast kinetics of oxygen reduction. The regenerated oxygen through the disproportionation of HO_2^- will be re-reduced on-site at the carbon electrode. Thus, a manganese oxide catalyst makes the oxygen reduction a pseudo 4-electron reduction by increasing the reduction current density via replenishment of oxygen through a catalyzed disproportionation of HO_2^-. Therefore, the reduction current increases at the manganese oxide catalyzed carbon electrode [12–14].

The argument, however, is whether or not MnO_2 participates in the 2-electron reduction process. Since the reduction potential of MnO_2 is close to the oxygen reduction potential in alkaline electrolyte, the reduction of the MnO_2 catalyst may occur at the same time as oxygen reduction or at a more positive potential due the high overpotential for the ORR. The mechanism for the catalytic oxygen reduction could be through the chemical oxidation of the reduction product of MnO_2. The electrocatalytic activity could be related to the occurrence of a mediation process involving the reduction of Mn(IV) and Mn(III), followed by the electron trans-

* Corresponding author. Tel.: +1 617 287 6035; fax: +1 617 287 6185.
E-mail address: deyang.qu@umb.edu (D. Qu).
[1] Summer intern from Lexington Public School, Currently School of Engineering and Applied Science, University of Pennsylvania, Philadelphia, PA, United States.

0378-7753/$ – see front matter © 2010 Elsevier B.V. All rights reserved.
doi:10.1016/j.jpowsour.2009.12.128

fer of Mn(III) to oxygen and by the disproportion reaction of the HO_2^- species in the manganese oxide sites [11,14]. Cao et al. [13] reported that the ORR happened in parallel with the reduction of MnO_2 to MnOOH, and the catalytic activity of MnO_2 is dependent on its electrochemical activity. However, after investigating the MnO_2 catalyzed ORR on a Nafion-modified gold electrode, Mao et al. proposed that MnO_x does not enhance the first 2-electron process of reducing O_2 to HO_2^- [12], and the oxygen reduction reaction may occur mainly on carbon sites [11]. In order to improve the kinetics of the 2-electron reduction of O_2, the same authors proposed a dual catalyst for redox-mediating O_2 reduction and disproportionating the reduction intermediates by using CoTAPc and MnOOH, respectively [17,18].

A catalytic ORR at the gas diffusion electrode (GDE) occurs on the surface of the porous electrode. The actual catalytic activity is determined by the numbers of active sites on the electrode surface. The present investigation is devoted to the study of the interaction between a manganese oxide catalyst and carbon support, and the "active sites" for the ORR. Qu [19] reported that the catalytic activities of non-catalytic activated carbon materials are related to the surface structure, and the ORR mainly occurs on the edge orientation of the graphite micro-domains.

2. Materials and methods

2.1. Materials

The high surface area activated carbon materials UMB1-5 were home-made by the modification of commercial activated carbon materials, which were the same materials used in our previous publication [19]. ACS grade (99.0% min) $KMnO_4$ was purchased from VWR.

2.2. Catalyst loading into carbon matrix

There are two different ways to load solid MnO_2 catalyst into high surface area carbon materials. It can be done either by mechanically mixing the already prepared catalyst with carbon support or by impregnating soluble Mn species into the pores of the carbon material, followed by treatments to yield the MnO_2 catalyst. The advantage of the impregnation method is achievement of a homogeneous, highly dispersed catalyst on the surface of high surface area carbon electrodes. For example, in the studies reported by Zhu et al. [20], the meso-porous carbon was first made to become hydrophilic by surface modification, the liquid droplets with Mn(II) were introduced by adjusting the hydrophobic property and/or pore size of the carbon material. The $KMnO_4$ solution was then introduced to the pores of the carbon material. At last, MnO_2 nanoparticles with a typical size of 2–3 nm were formed within the pores of the carbon matrix after the permanganate was reduced by carbon. A systematic study was done by Qu and co-workers to optimize MnO_2 loading procedures by means of statistical Design-of-Experiment [21]. The process used to make the electrode for this study was the best one reported in reference [21].

MnO_2-loaded carbon material was made by reacting 80 mL of 2 wt% $KMnO_4$ solution with 50 g of carbon material suspended in 200 mL deionized (DI) water at 80 °C for 40 min. The catalyst-loaded carbon was then filtered, washed with DI water and dried overnight at 120 °C.

The content of the MnO_2 catalyst in the carbon matrix was analyzed by first digesting the MnO_2-loaded carbon in 10% HNO_3 solution at boiling temperature. MnO_2 was then reduced to soluble Mn^{2+}. The Mn^{2+} concentration in the solution was measured using Inductively Coupled Plasma (ICP).

2.3. Electrolyte, reference and counter electrodes

30 wt% aqueous KOH solution was used as an electrolyte in all experiments. All potentials reported were referred to the Hg/HgO reference electrode immersed in the electrolyte. A Ni-mesh was used as the counter electrode.

2.4. Construction of electrodes and electrochemical cell

The GDE was made with 90 wt% catalyst-loaded carbon material and 10 wt% Teflon® dry material. The Teflon® suspension (T-30) used was from DuPont. The catalyst-loaded activated carbon was first wet with iso-propanol solution and then mixed thoroughly with T-30. The dough was subsequently hot-rolled into a thin film and then hot-pressed onto a Ni-mesh current collector using a hydraulic press.

The construction of the electrochemical cell was reported in the previous publication [19]. The interfacial area between the GDE and the electrolyte was 95 mm^2.

Solid pyrolytic graphite rods (high order pyrolytic graphite (HOPG)) were sealed in shrinkable tubing. The surface of the edge orientation was polished to a mirror finish with a 3-μm polishing paper. The fresh surface of a basal orientation was revealed by placing a piece of Scotch® tape in contact with the basal surface and then peeling off a thin layer with the tape. One droplet of 2 wt% $KMnO_4$ was dropped on the surface of the graphite rods. After 1 h, the electrodes were immersed in a basic solution (pH 10, made with KOH), in order to wash away un-reacted permanganate from the surface without dissolving MnO_2. When the solid graphite rods were used as the working electrodes, they were housed in a three-neck flask. Pure oxygen or argon was bubbled through a sintered disperser for 1 h before the electrochemical measurements were conducted. The interfacial area of the graphite rod was 79 mm^2.

2.5. Experimental techniques and instrumental details

Electrochemical measurements were carried out using an EG&G 173 potentiostat/galvanostat controlled by a Q&R Smart Data Package. A Micromeritics ASAP 2020 porosimeter was used for measuring the surface area and porosity. Nitrogen was used as an adsorbate gas. Density Functional Theory (DFT) software from Micromeritics was used for the calculation of pore distribution. Slit-pore geometry was assumed. A Perkin Elmer Optima 3000XL ICP Spectrometer was used for the analysis of soluble Mn^{2+}

3. Results and discussion

3.1. Reduction of oxygen on the basal and edge orientations of HOPG coated with MnO_2 catalyst

The carbon active site for the reaction has been determined to be the edge orientation of the carbon [19]. However, for the GDE loaded with MnO_2 catalyst, the catalytic activity of the carbon material, the contribution of a MnO_2 catalyst, and interaction between MnO_2 and carbon should be taken into consideration. In order to investigate the oxygen reduction mechanism and the active site for a carbon electrode loaded with MnO_2, the ORR on the edge and basal surface of HOPG coated with MnO_2 was studied. HOPG is a very well crystallized graphite; its basal orientation is flat on the atomic scale and can be considered a nearly defect free surface. Fig. 1 shows the comparison of the cyclic voltammetry for the basal and edge planes coated with MnO_2 catalyst in argon. They were the typical profiles for the reduction of MnO_2 [20]. Obviously, the amount of MnO_2 on the surface of the edge orientation was significantly higher than that on the basal plane. The chemical properties of the basal and edge orientations are significantly

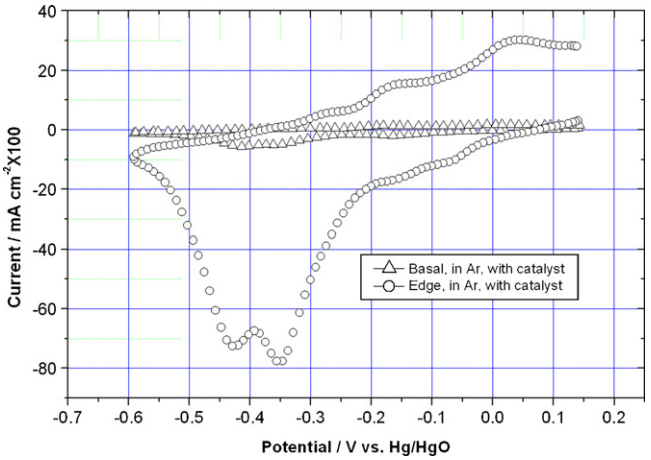

Fig. 1. Cyclic voltammetry for the reduction of MnO_2 loaded on the edge and basal orientations of HOPG in the electrolyte saturated with argon. Scan rate: 0.1 mV s^{-1}.

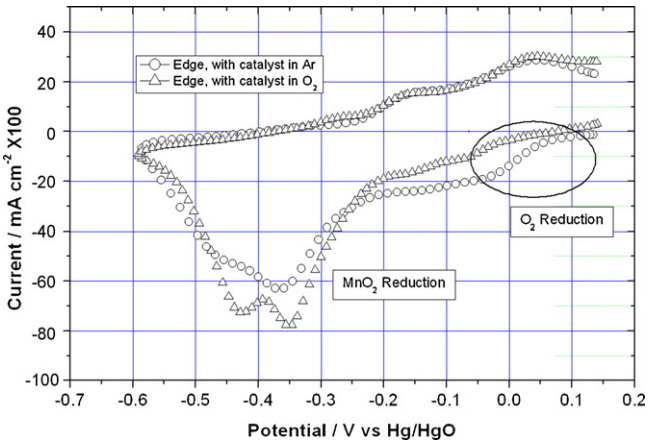

Fig. 3. Cyclic voltammetry at MnO_2-loaded edge plane in argon and oxygen saturated electrolyte. Scan rate: 0.1 mV s^{-1}.

different. There are no unsaturated chemical bonds, free electrons or chemically bonded functional groups on the basal plane, making it resistant to oxidation. The edge plane, however, is rough with unsatisfied valences. Most of the surface functional groups are attached to it, so it is more chemically active than the basal plane. The MnO_2 catalyst was loaded on the graphite surface by reacting $KMnO_4$ with carbon. $KMnO_4$ would be reduced to MnO_2 while carbon would become oxidized to CO_2. It appears that only a limited amount carbon (maybe a few layers of carbon on the surface) became oxidized on the basal surface, and much more carbon was oxidized on the edge layer, allowing a larger deposition of MnO_2 on the edge orientation.

Fig. 2 shows the potentiodynamic analysis of the ORR on the basal and edge orientations catalyzed with MnO_2. A significant difference can be observed. The catalytic reduction of oxygen was inhibited on the basal plane, and the edge orientation demonstrated a high activity. The results were consistent with the oxygen reduction on pyrolitic graphite [20,22–24]. Figs. 1 and 2 seem to demonstrate that the majority of MnO_2 would be deposited on the edge plane, and the catalytic activity of the edge orientation is much higher than that of the basal plane. Fig. 3 shows the cyclicvoltammetry profiles for the edge plane loaded with catalyst in the electrolyte saturated with O_2 or Ar. Apparently, the reduction of MnO_2 on both electrodes happened in the same potential range (−0.2 V to −0.5 V vs. Hg/HgO reference electrode), which is

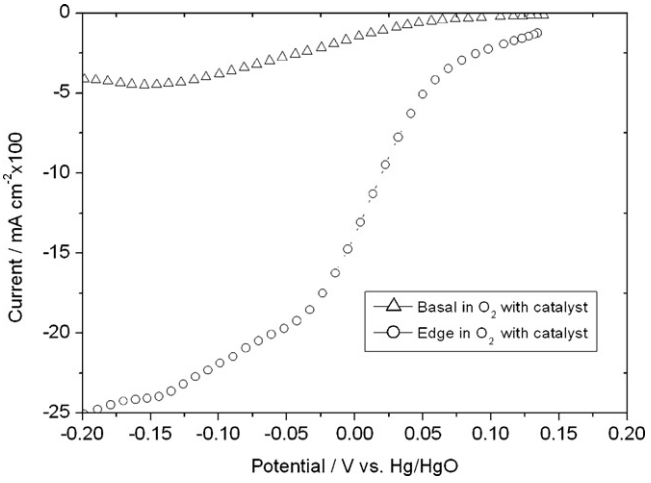

Fig. 2. Potentiodynamic curve for O_2 reduction at MnO_2-loaded edge and basal layers of HOPG. Scan rate: 0.1 mV s^{-1}.

about 250 mV more negative than the ORR potential (0.0–0.1 V vs. Hg/HgO). Even though there might be some high oxidation state Mn being reduced at more positive potentials, the majority of the MnO_2 was reduced after the ORR happened. Thus, the mechanism involving Mn^{4+}/Mn^{3+} mediation process is difficult to reconcile in this case since the Mn^{4+} formed by the reaction between permanganate and carbon would gain one electron at a much more negative potential than that of the ORR. Zoltowsi et al. [24] reported that the addition of moderate quantities of MnO_2 powder gave a beneficial effect in the region of high currents, and 80% of MnO_2 was used in the catalyst layer in Cao et al.'s report [13]. In both reports, MnO_2 was mechanically mixed with the carbon materials. It would be difficult for the powdered MnO_2 to gain intimate contact with different carbon orientations. So, the good initial performance may result from the reduction of highly active powdered MnO_2 rather than the catalytic reduction of oxygen. Indeed, some forms of highly active MnO_2, e.g. γ-MnO_2, which is commonly used in primary alkaline MnO_2/Zn cells, would become reduced at a more positive potential than oxygen. The hypothesis is consistent with what Cao et al. [13] reported: that the catalytic activity of MnO_2 is closely related to the electrochemical activities of MnO_2.

Fig. 4A and B shows the comparison of the ORR on the catalyzed and non-catalyzed edge and basal planes, respectively. Fig. 4A shows the significant increase of the reduction current for the MnO_2-loaded edge electrode. However, it is interesting to point out that the ORR overpotential remained almost the same in the both cases. If the catalyzed 2-electron reduction involves a Mn^{4+}/Mn^{3+} mediation process, then the ORR overpotential would decrease on the MnO_2-loaded surface. The significant increase of the reduction current could result from the replenishment of oxygen through the catalyzed disproportionation of HO_2^-. If the ORR on the MnO_2-loaded surface involves the formation of HO_2^- on carbon and then the disproportionation of HO_2^- on MnO_2, the current would just be doubled in the absence and in the presence of MnO_2. It is worth pointing out that the increase of the reduction current for the MnO_2-loaded electrode was larger than two times of that for the unloaded electrode. The phenomenon could result from the kinetic limitation on the carbon electrode due to the accumulation of peroxide on the surface. Fig. 4B shows the comparison of the catalyzed and non-catalyzed basal planes. It is worth emphasizing that even though oxygen did not get reduced on the pristine basal plane, a small but significant ORR current can be observed on the MnO_2-loaded basal layer. The hypothesis is that permanganate may not react with carbon layer by layer on the basal plane, so local edge-like defects may be created during the catalyst loading, allowing the ORR to happen on those defects.

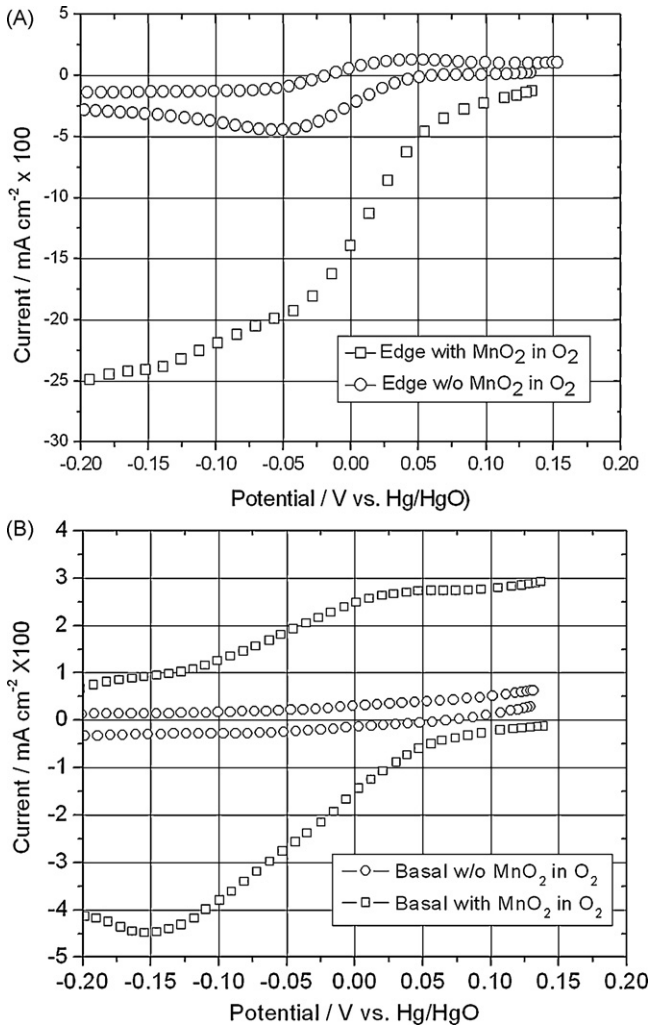

Fig. 4. Portions of cyclic voltammetry at (A) pristine and MnO_2-loaded basal planes and (B) pristine and MnO_2-loaded edge layers, both in O_2 saturated electrolyte. Scan rate: 0.1 mV s^{-1}.

3.2. ORR on the activated carbon electrode loaded with MnO_2 catalyst

Activated carbons contain pores starting from less than one nanometer to several thousand nanometers. The pores of different sizes play specific roles in the adsorption process. The adsorption isotherm gives useful information for the determination of the surface area of the adsorbent, the volume of the pores and their size distribution. Pores that have openings smaller than the size of a N_2 molecule or that do not have openings to the outside of the grains are not accessible to nitrogen adsorbate. The pore that is not accessible to a given adsorbate is referred as closed porosity. The surface area of the closed pores cannot be measured by physical adsorption. Understandably, most of the closed pores are micropores. The mechanism of the reaction between $KMnO_4$ and activated carbon was studied in detail in our previous publication [21]. $KMnO_4$ oxidizes the surface layer of carbon forming CO_2, while MnO_2 fine particles precipitate on the carbon surface. Such reaction could modify the carbon surface in two-way: first, when the permanganate reaches the carbon atoms on surface, the top layer of carbon will be removed by being oxidized to carbon dioxide, this processes happens on the external surface and within the large pores through which permanganate can reach the internal carbon surface of such pores, because permanganate ions can only penetrate large pores; second, the MnO_2 fine particles that are formed will precipitate on the surface of carbon where the redox reaction happens. Thus, solid MnO_2 would mainly deposit on the walls of the large pores which will reduce the surface area of large pores. Meanwhile, removing of the top carbon layers would reveal those otherwise seal-off pores and widen the opening of nano-pores. Therefore, the surface area of the initially closed pores which had not been available to N_2 adsorbate, or the nano-pores with the openings too small to accommodate N_2 absorbate, become accessible to the absorbate gas. The "adsorption" porosity could be modified. The composition of the MnO_2-loaded activated carbon materials is given in Table 1. The morphological parameters of the materials are also tabulated in the table in comparison to those of blank activated carbon materials. Although the change of total surface area after catalyst loading varied, the surface area of pores <7 Å increased and the surface area of pores >15 Å decreased for all five carbon materials, as demonstrated in Table 1. Fig. 5 shows the comparison of pore distribution for UMB5 activated carbon before and after catalyst loading. The change in porosity is clearly illustrated. The results were not only consistent with what we concluded in the previous publication [21], but explained what Zoltowsi et al. [24] observed. They both reported that a high relative discharge capacity was obtained for the electrode prepared with the low permanganate content at the high discharge rate. It is worth pointing out that the surface area reported in Table 1 was the surface area of powders. It would be useful to report the surface area of GDE directly, however, in order to obtain high quality and reproducible absorption data for a high surface area micro-porous carbon, the specimen needs to be degassed at relative high temperature in which Teflon becomes unstable.

Table 1
Comparison of the percentage of MnO_2, surface area, surface area of carbon, surface area of pore <7 Å, <15 Å, and >15 Å, and average pore size.

Sample	% MnO_2	Surface area (m^2 g^{-1})	Surface area of carbon (m^2 g^{-1})[a]	Surface of pore <7 Å (m^2 g^{-1})	Surface of pore <15 Å (m^2 g^{-1})	Surface of pore >15 Å (m^2 g^{-1})	Average pore size (Å)
UMB1		941		300	695	246	27.3
Mn-UMB1	1.9	859	874	406	700	159	25.0
UMB2		783		420	620	163	54.6
Mn-UMB2	1.9	784	798	560	710	74	40.4
UMB3		1211		450	900	311	24.6
Mn-UMB3	2.2	805	821	300	620	185	23.2
UMB4		717		320	617	100	36.9
Mn-UMB4	2.0	730	744	446	670	60	28.7
UMB5		904		385	690	215	31.9
Mn-UMB5	2.1	824	841	460	681	143	25.4

[a] The surface area of carbon was calculated based on the assumption that the surface area of MnO_2 is 50 m^2 g^{-1}. The rational for the assumption was discussed in detail in reference [21].

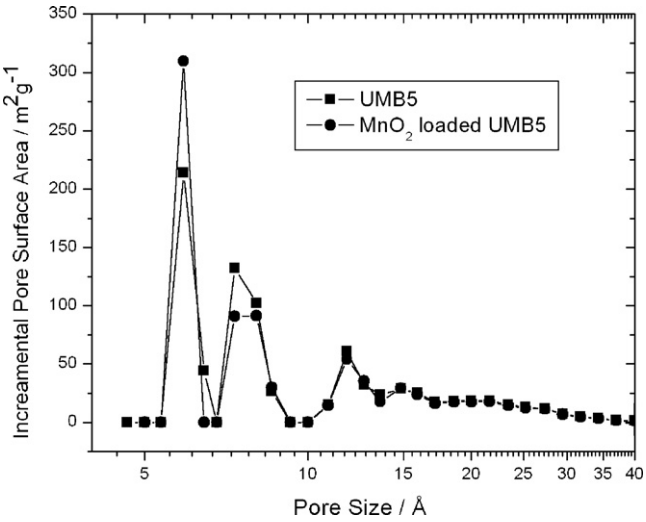

Fig. 5. Comparison of pore size distribution of blank and MnO_2-loaded activated carbon UMB5.

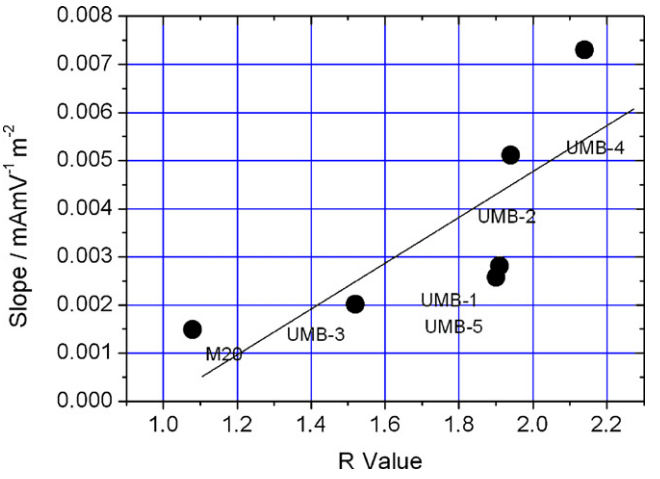

Fig. 7. Catalytic activity (the slope of potentiodynamic reduction curves as shown in Fig. 6) as a function of *R* value.

The specific surface area and porous structure of carbon materials are very important for the electrocatalytic performance of carbon supported catalysts. The higher electrocatalytic performance of a GDE could arise from the extension of the reaction zone. In other words, the unique structure of the MnO_2-loaded carbon matrix can provide more effective three-phase interface areas that increase the utilization of catalyst particles. Theoretically, the pores which can accommodate N_2 adsorbate at 77 K would be available for simple hydrated ions in alkaline electrolyte eventually [25]. However, in a GDE, the effective pores need to be large enough not only to accommodate the simple hydrated ions, dissolved O_2, and solvated anion intermediates, e.g. HO_2^-, but also to provide a fast mass transfer pathway. Appleby et al. suggested that a pore diameter in the order of 18 Å would be required to facilitate an effective ORR [26]. The ORR is a surface phenomenon, and the polarization is closely related to the local current density (mA per square meter of effective electrode area), thus a specific current density ought to be used in order to compare the catalytic activity of the carbon electrodes with different surface areas. Fig. 6 shows the potentiodynamic profiles taking into consideration the effective surface area.

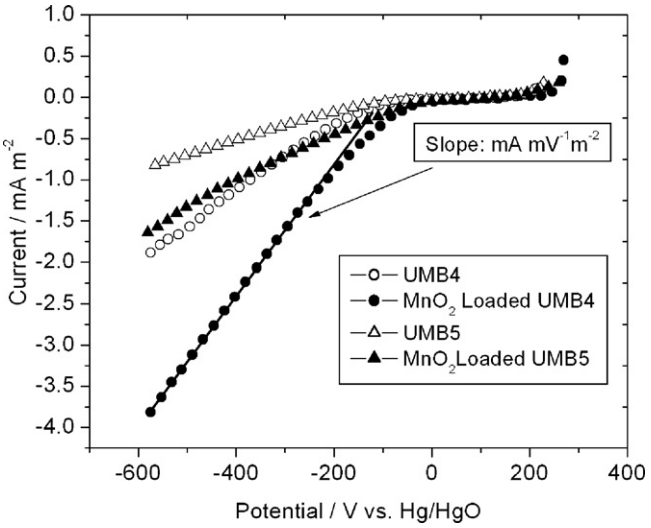

Fig. 6. Potentiodynamic for O_2 reduction at pristine and MnO_2-loaded UMB4 and UMB5 activated carbon materials. Surface area of pores with size larger than 15 Å was used to calculate the current density. Scan rate: 0.5 mV s^{-1}.

The surface area of the pores larger than 15 Å was assumed as an effective surface for the ORR [19]. Significant differences can be observed for the blank carbon electrodes and MnO_2-loaded electrodes. The addition of a very small quantity of manganese in the form of permanganate appreciably lowered the electrode polarization over the whole current density range.

The potential of the ORR results from IR drop, electrochemical polarization and mass transfer polarization. The electrocatalytic activity increases with the amount of the effective active sites on the surface of the porous electrode, which should be accessible to both electrolyte and oxygen in the gas phase. Without a sufficient supply of such active sites, lower potential resulted from kinetic limitation, and peroxide accumulation could occur.

The structure of activated carbon is composed of roughly parallel associations of hydrocarbon moieties and quite defective non-planar, but parallel, associations of carbon atoms [27]. Such short-range arrangements of the defective graphene sheets can be estimated by an empirical parameter (*R*), which is defined as the ratio of the height of the (0 0 2) Bragg peak to the background [28]. The *R* value is proportional to the average number of graphene layers stacked in parallel fashion, thus it is proportional to the amount of the edge orientation on the carbon surface. Larger *R* values indicate a higher percentage of edge orientation. Fig. 7 shows the relationship of the *R* value with the slope of the reduction curve (mA m^{-2} mV^{-1}). It is obvious that the specific catalytic activity of MnO_2-loaded carbon electrodes was significantly improved compared to that of the blank carbon electrodes. Similarly with blank activated carbon [19], the specific catalytic activity of MnO_2-loaded carbon electrodes increases as *R* increases, therefore it could be concluded that the MnO_2 catalyzed ORR mainly happens at the edge orientation of the activated carbon substrate. MnO_2 fine particles should disperse well over the surface of carbon materials. However, as concluded in Section 3.1, most of the MnO_2 particles are believed to be deposited on the edge orientation, which is in agreement with the ability of metal nanoparticles to form π-complexes with multiple –C–C– bonds at the edge of graphene networks [29]. In addition, one may also realize that the catalytic activity of MnO_2-loaded carbon electrodes with larger *R* values improved more against the blank carbon electrodes than those with smaller *R* values, as seen when comparing Fig. 7 with Fig. 7 in reference [19]. So, the 2-electron reduction of O_2 is proposed to happen on the edge orientation. MnO_2 nanoparticles, which may also accumulate at the edge plane, would catalyze the disproportionation of HO_2^-, and the additional O_2 would be reduced at the edge plane.

It is worth pointing out that the actual catalytic activity of a MnO_2-loaded carbon material is proportional to both the specific catalytic activity (per square meter), which is related to the concentration of edge orientation, and the effective surface area where the ORR takes place. It seems that while the specific catalytic activity increases with the help of the MnO_2 catalyst, the effective surface area, which is composed of the external surface and the surface of large pores, decreases due to the MnO_2 deposition. The process to make a good GDE would be to uniformly dope the surface of a high surface area carbon with a high percentage of large pores and of edge orientation with MnO_2 without significantly sacrificing the effective interfacial surface area.

4. Conclusions

The activity of MnO_2 loaded on HOPG electrodes was investigated. The amount of MnO_2 deposited on the edge layer is significantly higher than that on the basal layer. MnO_2 has limited impact on the 2-electron reduction of oxygen, which is believed to happen on the edge orientation of carbon, but it increases the reduction current density by replenishing additional oxygen through catalyzed disproportionation of HO_2^-.

Both effective interfacial surface area and specific catalytic activity for the MnO_2-loaded activated carbon materials were also investigated for the ORR. The specific catalytic activity of MnO_2-loaded carbon materials was found to rely on the active sites in the form of edge orientations on the carbon surface. MnO_2 nanoparticles were proposed to be mainly deposited on the edge surface. As the concentration of edge orientation increased, the specific catalytic activity also increased. The edge orientation with the deposition of MnO_2 on the surface of the activated carbon substrate serves as an "active site" for the ORR. The total interfacial area is dependent on the percentage of large pores. The surface area of smaller pores increased and the surface area of larger pores decreased after the carbon materials reacted with $KMnO_4$. The redox reaction between the carbon and permanganate may open up closed pores by removing the surface carbon layer, and MnO_2 may be deposited mainly on the external surface and surface of large pores.

Acknowledgment

The work was supported by the Assistant Secretary for Energy Efficiency and Renewable Energy, Office of Vehicle Technologies, under the program "Hybrid and Electric Systems," of the U.S. Department of Energy under Contract Number DEAC02-98CH10886.

References

[1] G.Q. Zhang, X.G. Zhang, Electrochim. Acta 49 (2004) 873–877.
[2] G.Q. Zhang, X.G. Zhang, Y.G. Wang, Carbon 42 (2004) 3097–3102.
[3] M.S. El-Deab, T. Ohsaka, Electrochim. Acta 52 (2007) 2166–2174.
[4] J. Vondrak, B. Klapste, J. Velicka, M. Sedlarikova, J. Teiter, I. Roche, E. Chainet, J.F. Fauvarque, M. Chatenet, J. New Mater. Electrochem. Syst. 8 (2005) 209–212.
[5] W.Z. Zhu, B.A. Poole, D.R. Cahela, B.J. Tatrachuk, J. Appl. Electrochem. 33 (2003) 29–36.
[6] Z.D. Wei, W.Z. Huang, S.T. Zhang, J. Tan, J. Appl. Electrochem. 30 (2000) 1133–1136.
[7] Z.D. Wei, W.Z. Huang, S.T. Zhang, J. Tan, J. Power Sources 91 (2000) 83–85.
[8] Y.G. Wang, L. Cheng, F. Li, H.M. Xiong, Y.Y. Xia, Chem. Mater. 19 (2007) 2095–2101.
[9] K. Gong, P. Yu, L. Su, S.X. Xiong, L.Q. Mao, J. Phys. Chem. C 111 (2007) 1882–1887.
[10] D. Zhang, T. Sotomura, T. Ohsaka, Chem. Lett. 35 (2006) 520–523.
[11] F.H.B. Lima, M.L. Calegaro, E.A. Ticianelli, Electrochim. Acta 52 (2007) 3732–3738.
[12] L. Mao, D. Zhang, T. Sotomura, K. Nakatsu, N. Koshiba, T. Ohsaka, Electrochim. Acta 48 (2003) 1015–1021.
[13] Y.L. Cao, H.X. Yang, X.P. Ai, L.F. Xiao, J. Electroanal. Chem. 557 (2003) 127–134.
[14] F.H.B. Lima, M.L. Calegario, E.A. Ticianelli, J. Electroanal. Chem. 590 (2006) 152–160.
[15] M.L. Calegaro, F.H.B. Lima, E.A. Ticianelli, J. Power Sources 158 (2006) 735–739.
[16] L. Mao, T. Sotomura, K. Nakatsu, N. Koshiba, D. Zhang, T. Ohsaka, J. Electrochem. Soc. 149 (2002) A504–A507.
[17] L. Mao, K. Arihara, T. Sotomura, T. Ohsaka, Chem. Commun. (2003) 2818–2820.
[18] T. Ohsaka, L. Mao, K. Arihara, T. Sotomura, Electrochem. Commun. 6 (2004) 273–277.
[19] D. Qu, Carbon 45 (2007) 1296–1301.
[20] S. Zhu, H. Zhou, M. Hibino, I. Honma, M. Ichihara, Adv. Funct. Mater. 15 (2005) 381–386.
[21] N. Ohimde, N. Bartlett, X.Q. Yang, D.Y. Qu, J. Power Sources 185 (2008) 747–753.
[22] E. Yeager, P. Lrouse, K.V. Rao, Electrochim. Acta 9 (1969) 1057–1070.
[23] I. Morcos, E. Yeager, Electrochim. Acta 15 (1970) 953–975.
[24] P. Zoltowsi, D.M. Drazic, L. Votrkapic, J. Appl. Electrochem. 3 (1973) 271–283.
[25] A. Soffer, N. Folman, J. Electroanal. Chem. 38 (1972) 25–43.
[26] A.J. Appleby, J. Marie, Electrochim. Acta 24 (1979) 195–202.
[27] H. Marsh, F. Rodrigues-Reinoso, Activated Carbon, Elsevier, New York, 2006.
[28] Y. Liu, J.X. Xue, T. Zheng, J.R. Dahn, Carbon 34 (1996) 193–200.
[29] W.M.H. Sachtler, A.V. Stakheev, Catal. Today 12 (1992) 283–295.